ARPN Journal of Engineering and Applied Sciences

NUMERICAL ANALYSIS OF REINFORCED LIGHTWEIGHT AGGREGATE CONCRETE HOLLOW CORE SLABS

Adel A. Al-Azzawi and Basma M. Abdul Al-Aziz
Department of Civil Engineering, Factually of Engineering, Al-Nahrain University, Baghdad, Iraq
E-Mail: dr_adel_azzawi@yahoo.com

ABSTRACT

Two types of reduction in weight can be obtained for a slab. The first is by using lightweight aggregate concrete and the second is obtained through changing the geometry of cross sectional area of slabs for example hollow core slabs and ribbed slab. In this research, two types of reduction in weight can be obtained. The first by using lightweight coarse aggregate (crushed brick) and second is by using hollow core. As a result of reducing the own weight of slabs in the building, the cost of the structure will be reduced. These slab specimens were analyzed numerically by using the finite element computer program ANSYS with dimensions (1.1m) length, (0.6m) width and (120mm) thickness. The specimens are divided into two lightweight aggregate solid slabs with varying shear span to effective depth value, one normal aggregate solid slab with shear span to effective depth equal (2.9), two lightweight aggregate hollow circular core slabs (HCCS) with core diameter (50mm) with varying shear span to effective depth value , one lightweight aggregate hollow square core slabs (HSCS) with core side length (50mm) and shear span to effective depth equal (1.9) and one normal aggregate (hollow circular core slab) with core diameter (50mm) and shear span to effective depth equal (2.9). In this research, the maximum reduction in weight due to aggregate type was (19.28%) and due to cross section (square and circular) cores was (17.365 and 13.64%) respectively. The results of analysis showed good agreement with the experimental test results with variation of (7.56%) in ultimate strength and (7.26%) in deflection. A parametric study have been implemented by using ANSYS program to investigate the effect of number, diameter and area of cores , effect of load Location, effect of adding top steel reinforcement, effect of the distance between applied load and supports and effect of top reinforcement on mode of failure.

Keywords: ANSYS, finite element, hollow core, lightweight aggregate, numerical, reinforced concrete slab.

INTRODUCTION

The reduction of building weight is achieved through reduction in material weight or reduction in section mass. Lightweight aggregate is used in construction manufacture for a variety of uses for example lightweight fill behind retaining walls and over utility pipelines in unearthed trenches, masonry block, structural concrete, and pavement. Structural lightweight aggregates (SLWA) are produced in manufacturing plants from raw materials, including appropriate shale's, clays, slates, fly ashes, or blast-furnace slag. Normally happening of lightweight aggregate are mined from volcanic stores that include pumice and scoria [1].

The primary specialties of lightweight concrete (LWC) are its low density and thermal conductivity. Its advantages are that there is decreases of dead load, speedier building rates in construction, bring down haulage and taking care of expenses.

Slabs are built in large diversity of methods such as in-situ, precast or composite with a large diversity of structural forms such as solid, hole, ribbed, and waffle. Hollow core slab (HCS) is a concrete slab provided to lessen weight and, consequently, cost and, as a part advantage, to use for hid electrical or mechanical runs. Fundamentally used as roof or floor deck systems. Hollow core slab likewise have applications as bridge deck units and spandrel members.

a) Structural lightweight aggregate concrete by using crushed clay brick

In 2009, Fadia S. Kallak [2] studied the possibility of using crushed bricks as coarse aggregate in concrete. First concrete mixing was without use of crushed bricks and adopted mixture reference for the purpose of comparing the results. The second mixture was prepared using different ratios of crushed bricks for the weight of coarse aggregate. 30 model of concrete was prepared with and without crushed brick and models were examined under the influence of compression load and carrying indirect tensile test according to the requirements of British specifications and results show that the use of crushed bricks led to reduce the resistance of concrete in addition to that the percentage of water has increased. The main conclusions were:

a) The crushed bricks can be utilized satisfactory as rough aggregate for manufacture concrete of agreeable strength characteristics.

b) The utilization of crushed bricks as coarse aggregate reduce the compressive strength of concrete around (11-87) % as per to the proportion of used crushed bricks.

c) The workability of the crushed bricks concrete is lower than that of normal concrete.

d) The splitting tensile strength (f `ct) of crushed brick concretes is lower than that of normal concrete. The proportion ranged from (0.2-1.4).

e) The use of crushed bricks as coarse aggregate in concrete rise water cement ratio (w/c) as it increased the absorption of concrete to the water.

In 2011, Ghazi [3] studied the characteristic of hardened concrete using of crushed clay brick. Eight vary crushed clay brick aggregate concretes were utilized. Pulse velocity, splitting tensile and compressive strength of crushed clay brick aggregates concrete were resolved and compared to normal aggregate concrete (NAC) result. The splitting tensile test (f `ct) of crushed clay brick were permanently lower than normal aggregate concrete (NAC), the reducing in splitting tensile strength of crushed clay brick is ranging between 11 and 26% with an average reduction of about 18.5% compared to NAC. The compressive strength (f `c) of crushed clay brick aggregates concretes were always lower than the compressive strength (f `c) of NAC in any way the age of concrete, but the crushed clay brick aggregates concrete displayed better implementation as the period of concrete increments and average reduction in compressive strength were 33.5% at the age of 7 days.

In 2016, Yousif Khalaf [4] carried out an experimental and numerical investigation on the behavior of self compacting lightweight aggregate (LWA) reinforced concrete thick slabs. The experimental work procedure consisted of testing twenty one reinforced concrete slabs with and without opening. All specimens have the same flexural reinforcement and planar dimensions (1000x1000mm) with three different thicknesses of (120mm, 100mm, and 80mm). The investigated test parameters were slab thickness, opening shape, and opening size. Waste brick bits were crushed and used as recycled lightweight coarse aggregates. It was concluded that, with increasing the slab depth the cracking and the ultimate loads increased. Also, the ratio of first cracking load to ultimate load increased according to slab depth. Numerically the finite element method by using ANSYS computer program was used to study the performance of these reinforced concrete slabs.

b) Structural hollow core slabs

In 2006, Al-Maleki [5], studied the presences of voids in slabs. A linear analysis using the PLA computer program was grown based on the proposed method suggested through Stanton [6] and nonlinear three-dimensional numerical analysis have been utilized to predict the load–deflection performance of reinforced concrete slabs with hollow core (HC) using (ANSYS V.5.4) software. The 8-node brick element and the 6-node wedge element are utilized to represent the concrete. The reinforcing steel bars are modeled as discrete elements or supposed to be smeared through the element. Three slabs were analyzed with and without HC and a comparison was made with experimental load–deflection curves of these slabs. Good agreement with the experimental results was observed. Parametric study to investigate the effect of voids on the behavior of reinforced concrete slabs such as the effect of increasing compressive strength of concrete, the amount of steel reinforcement present in the slabs, shape, number and diameter of voids on the response of reinforced concrete slabs. The results showed that the utilize of square or rectangular shape voids reduces the ultimate strength by about 2.8% and 14.7%. It was also noticed decrease the stiffness and the ultimate load capacity when using (3 or 4) voids instead of (2) voids by about 3.9% and 2.2%.

In 2009, Qaqish *et al*. [7] presented an analysis of voided slab bridge deck. The voided slab is consisted of 200mm bottom and top slabs with diameter of circular voided equal 500mm and the distance center to center of these circles 750mm. A voided slab consisted of (2) continuous span (16m) width and (17.3m) Long with depth (0.9m). Two techniques are implemented for analysis the bridge deck. (AASHTO) specifications is the first one where (1) dimensional technique is depended and the second is (3) dimensional techniques where numerical analysis is regarded. The positions of (AASHTO) loadings are located at assured points to give max. negative and positive shearing. These positions are decided from (1) dimensional specimen. They deduce the max. shears got by two techniques are found to be in good correspond with disregard variances, and the results of the max. shears and the bending moments vary nearly 3% (finite element smaller than AASHTO).

In 2011, Mahdi [8], carried out nonlinear analysis of reinforced concrete hollow core slab (HCS) numerically using beam elements and plate bending elements to model the structure. The main idea was to divide the hollow core slab into (2) major elements. Stiffening beams representing the vertical webs between the voids and hollow plates representing the lower and upper flanges. Computer software that was adjustment for analyzing different reinforced and pre-stressed concrete hollow core slab and finite element solutions were compared with the experimental results to display the potential of the computational nonlinear model.

In 2016, AL-Azzawi and Abed [9], carried out an experimental and a numerical investigations on the performance of reinforced concrete slabs having longitudinal hollow core with various volumes and with different loading conditions by varying the shear span to effective depth values. The experimental study included eight moderately thick reinforced concrete slabs. The dimensional of the slab models (2.05m) length, (0.6m) width and (0.25m) thickness. The results showed that the ultimate capacity decreased by about (21% and 33%) for solid slabs with increasing shear span to effective depth values from (2 to 3) respectively. The ultimate capacity of circular hollow cores reduced by about (5.49%, 15.7% and 20.6%) with using circular diameter (75, 100 and 150). When shear span to effective depth values increased from (2) to (2.5 and 3) respectively, the ultimate strength of hollow core slab decreased by (31% and 45%) respectively. Numerically the finite element method by using ANSYS computer program was used to study the behavior of these reinforced concrete slabs.

Based on previous studied the reduction in weight due to both material and cross section has not yet been investigated. In the present research, the two types of reduction weight for structure are achieved through using lightweight aggregate (LWA) and hollow cores (HC).

NUMERICAL ANALYSIS OF SLABS

A nonlinear finite element analysis has been done to analyze the reinforced lightweight aggregate hollow core slabs in this study. The analysis is carried out by using ANSYS software program (Version 11.0) [10].
A typical ANSYS analysis has major steps:

a) Definition the element types, real constant and properties of the material used.

b) Formation the model.

c) Applying the loads and boundary condition.

d) Presentation the results.

Element types

In the first step, the element types for each material used in the analysis were chosen. In this study, three element types were used. These elements are solid65 for representing concrete, link180 for representing steel reinforcement and solid185 for modeling rubber and steel plates that represent the supports and point of loading locations.

Solid65 element

Three dimensional brick element (Solid65) was utilized for modeling concrete and it has eight nodes with three degrees of freedom at every one node-translation in the nodal x, y and z directions. This element is capable of plastic cracking (in three orthogonal directions), crushing, creep and plastic deformation [10].

Link 180 element

The (link 180) is used to Model the steel reinforcement of tested slabs. The three dimensional spar element is a uniaxial tension-compression element with two nodes each node has with three degrees of freedom translations in the nodal (x, y, and z) directions. This element is also capable of plastic deformation [10].

Solid185 element

Solid185 was used for modeling steel supporting plates in the slabs models. This element is defined by eight nodes with three degrees of freedom at every one node translation in (x, y and z) directions [10]. Rubber and steel plates were used for modeling support and line of load positions in the finite element models (as in the actual slabs) to produce a uniform stress distribution over the rubber, support and areas of lines load with (15mm) thickness for support and line load and (10mm) for rubber. The steel plates were presupposed to be linear elastic materials.

Real constants

In the analysis, real constant set1 is set to zero for solid65 element, which requires real constants for smeared reinforcement in the three directions x, y and z because the reinforcement is treated as discrete representation. Real constant set2 refers to second element type link180, which represent the bar cross sectional area, and real constant set3 refers to second element link180 which represent the bar with half cross sectional areas as shown in Table-1.

Table-1. Real constant for reinforcement link180.

	Set No.	Definition	Value
Link180	2	Area of reinforcement (mm^2) for Ø8	50.3
	3	Area of reinforcement (mm^2) for Ø8	25.15*

* This set was used because only quarter of model was used in the analysis.

Material properties

For every one element, there is material properties behavior. Material properties number (1) refers to concrete element (solid65). This element requires linear elastic isotropic concrete properties (modulus of elasticity and Poisson's ratios), nonlinear concrete parameters and multilinear isotropic for normal aggregate concrete models. While the element requires for lightweight aggregate concrete models linear elastic isotropic concrete properties (modulus of elasticity and Poisson's ratios), nonlinear concrete parameters, multilinear isotropic and density. Material properties used in the analysis are shown in Table-2 and Table-3.

Material properties number (2) refers to the (link180) element for steel reinforcement representation. This element requires information regarding the linear isotropic and bilinear isotropic as shown in Table-4 for normal and lightweight aggregate reinforcement models.

Material properties number (3) refers to the solid185 element for steel plates were added at support and point of load location representation. This element requires linear elastic isotropic concrete properties (modulus of elasticity and Poisson's ratios) only shown in Table-5.

Material properties number 4 refers to the solid185 element for rubber representation. This element requires linear elastic isotropic concrete properties (modulus of elasticity and Poisson's ratios) only as shown in Table-6.

Table-2. Material properties for Solid65 element for modeling normal aggregate concrete.

Element	Parameter	Definition	Value
Solid65	E_c	Young's modulus of elasticity (MPa)	28135.7
	υ	Poisson's ratio	0.2*
	β_o	Shear transfer parameters	0.7*
	β_c		0.95*
	$f_c^{'}$	Ultimate compressive strength (MPa)	35.6
	f_t	Ultimate tensile strength (MPa)	3.37
	Definition of strain-stress relationship for concrete (multilinear isotropic)**		

Table-3. Material properties for Solid65 element for modeling lightweight aggregate concrete.

Element	Parameter	Definition	Value
Solid65	E_c	Young's modulus of elasticity (MPa)	19225
	υ	Poisson's ratio	0.2*
	β_o	Shear transfer parameters	0.7*
	β_c		0.95*
	$f_c^{'}$	Ultimate compressive strength(MPa)	27.7
	f_t	Ultimate tensile strength (MPa)	2.32
	Definition of strain-stress relationship for concrete (multilinear isotropic)***		
	Density	1917	

Table-4. Material properties for Link180 element for modeling reinforcement.

	Parameter	Definition	Value
Link180	F_y	Yield strength (MPa) for Ø8	548
	Es	Modulus of elasticity (MPa)	200000
	Et	Steel hardening (MPa)	20*
	υ	Poisson's ratio	0.3*

Table-5. Material properties for Solid185 element for modeling steel plates.

	Parameter	Definition	Value
Solid185	Es	Modulus of elasticity (MPa)	2000000*
	υ	Poisson's ratio	0.3*

Table-6. Material properties for Solid185 element for modeling rubber.

	Parameter	Definition	Value
Solid185	Es	Modulus of elasticity (MPa)	2*
	υ	Poisson's ratio	0.3*

VOL. 12, NO. 6, MARCH 2017 ISSN 1819-6608
ARPN Journal of Engineering and Applied Sciences

Note: All value in Tables (2 to 6) with (*) means assumed values.

Note: Values in Table-2 with (**) is obtained from the stress-strain relationship for the concrete model using the following equations to compute the multilinear isotropic stress-strain curve for the concrete [11]:

$$\boldsymbol{f_c = \frac{\varepsilon E_c}{1+\left(\frac{\varepsilon}{\varepsilon_o}\right)^2}} \tag{1}$$

$$\boldsymbol{\varepsilon_o = \frac{2f\grave{}_c}{E_c}} \tag{2}$$

$$\boldsymbol{f_c = \varepsilon E_c} \tag{3}$$

where:

f_c = Stress at any strain.

ε = Strain at stress f_c .

ε₀ = Strain at ultimate compressive strength f'_C .

As shown in Figure-1 the simplified stress-strain relationship used in this study is constructed from six points connected by straight lines. The first point is defined as (0.3 f'_C), and calculated at the linear range (equation 3). Points 2, 3, 4 and 5 are calculated from equation (1), while point 6 is at ε_o and f'_C .

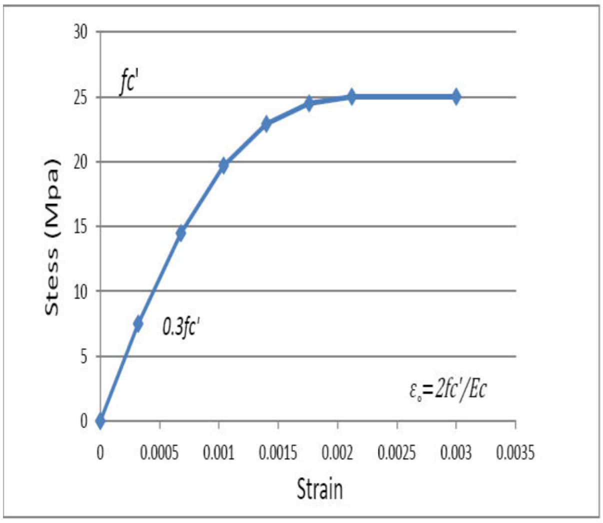

Figure-1. Simplified compressive uniaxial stress-strain curve for concrete [11].

Note: Values in Table-3 with (***) are obtained from experimental test [12].

Modeling of reinforced concrete slabs

All slabs had the same dimensions (1100mm) length (600) width and (120mm) thickness. The clear span between the two supports was (1000mm). The tested slabs were loaded using two line loads. Double symmetry of the tested slab are used because the solution takes a long time up to more than (15) hour when using full model in the analysis. Therefore only a quarter of slab was used for modeling the samples by ANSYS program and the solution takes only (30) min. The dimensions of quarter model used in ANSYS program have (550mm) length; (300mm) width and (120mm) thickness are shown in Figures (2) to (4). Seven samples were analyzed by ANSYS program included solids slab (normal concrete and lightweight concrete) with different a\d ratio (shear span to effective depth ratio), and hollow core slabs (normal concrete and lightweight concrete) with different a\d ratio, and different core shape additional to the study parameters.

The concrete model that represent the concrete slabs (normal concrete and lightweight concrete) with longitudinal HC or without it are expressed by forming areas at (x-y) plane and after that deduct the area of cores and then extrudes in (z-direction) in order to make the slabs volume. The reinforcement bars was created by element line attached at the concrete element nodes.

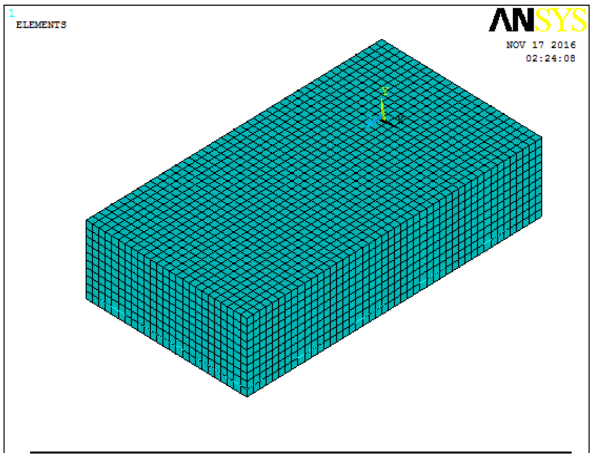

Figure-2. Mesh of quarter of solid slab.

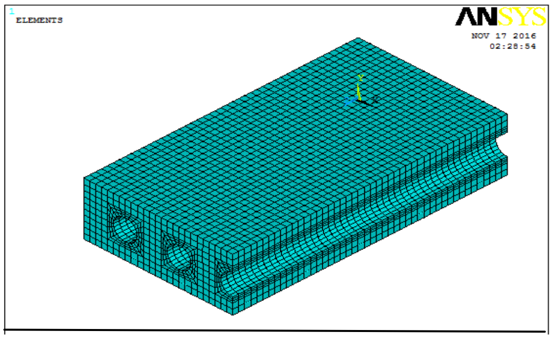

Figure-3. Mesh of quarter of hollow circular core slab.

ARPN Journal of Engineering and Applied Sciences

www.arpnjournals.com

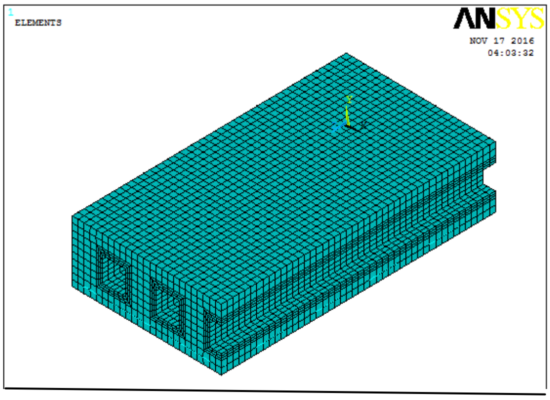

Figure-4. Mesh of quarter of hollow square core slab.

Steel reinforcement

The longitudinal and transverse reinforcement bars were formed as a net at bottom of the concrete slabs similar to that used in the experimental work. The discrete representation of bars is used to model reinforcement. The individual elements were created by using (Link180) element that passes through the nodes of the concrete elements for representing the reinforcement steel bars. The details of used reinforcement between concrete elements are shown in Figure-5 for quarter of slab model.

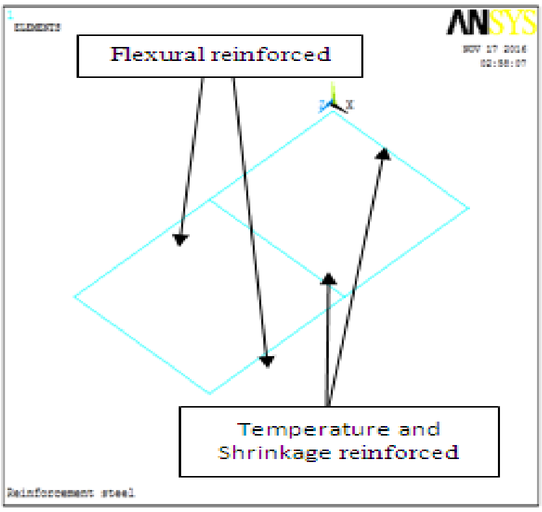

Figure-5. Steel reinforcement for quarter of slab model which is used in analysis.

Loading and boundary conditions

Due to utilize rubber parts at the positions of loading and supporting in the experimental slab samples. These rubbers can be redounding in some of deflection through the initial stage of loading. In order to have realistic modeling, the cushion in ANSYS modeling consists of two parts for the same element solid185 first part represent for rubber and second part represent for steel plates. Two cushions of (10mm) thickness were modeled using (Solid185) element to represent rubber, at the support, and two cushions at loading location. While two steel plates of (15mm) thickness were formed utilizing (Solid185) element, are placed at the support, and two steel plates at location of loading with same volume of concrete mesh (12mm) in order to a void stress concentration problems. This will provide a uniform stress distribution over the support area as shown in figure-6 for quarter of slab model.

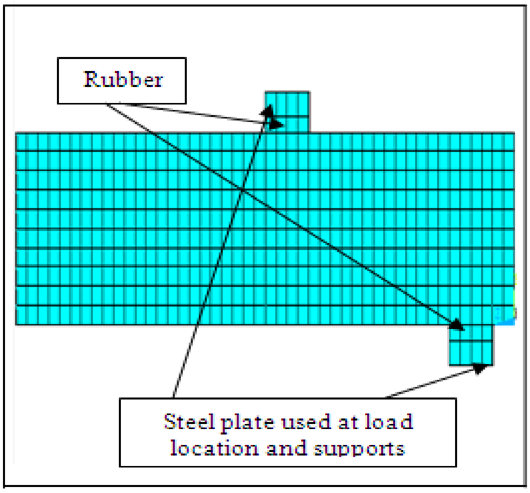

Figure-6. Rubbers and steel plates for quarter of slab model that used in analysis.

Presentation of the finite element analysis results

The experimental results [12] and nonlinear finite element analysis results by ANSYS package and were presented for solid and hollow core reinforced concrete slabs.

Table-7. Results of experimental work [12] and finite element analysis.

Modeled slabs	Type and Description	Shear span to effective depth (a/d)ratio	Ultimate load P_u (kN) in experimental work.	Ultimate load P_u (kN) by ANSYS	Difference %	Mid span deflection Δ_u(mm) in experimental work	Mid span deflection Δ_u(mm) by ANSYS	Difference %
Slab (1)	Normal aggregate solid slab	2.9	75.6	80.6	6.61	31.41	28.48	-9.33
Slab (2)	Lightweight aggregate solid slab	2.9	71.82	77.6	8.05	35.35	32.773	-7.29
Slab (3)	Lightweight aggregate solid	1.9	101.25	109.2	7.85	43.0	39.845	-7.34

ARPN Journal of Engineering and Applied Sciences

	slab							
Slab (4)	Lightweight aggregate hollow circular core slab	2.9	68.1	75.252	10.5	38.52	38.441	-0.21
Slab (5)	Normal aggregate hollow circular core slab	2.9	71.45	76.4	6.93	33.6	31.026	-7.66
Slab (6)	Lightweight aggregate hollow circular core slab	2.9	97.12	106.76	9.93	46.6	43.83	-5.94
Slab (7)	Lightweight aggregate hollow square core slab	1.9	73.21	71.0	3.02	12.35	10.735	-13.08
					7.56			7.26

Load-deflection behavior

The vertical deflection in Y-direction is produced under the load at the bottom face of the slab and at the mid span. Deflection behavior of numerical analysis of slabs due to the applied loading is shown in Figures (7) to (13). It is obvious that all slabs with shear span to effective depth ratio equal to 2.9 have similar general behavior with small difference in the value of maximum deflection. For the shear span to effective depth ratio equal to 1.9 the slab7 show different behavior because the mode of failure is different (hollow square core slab).

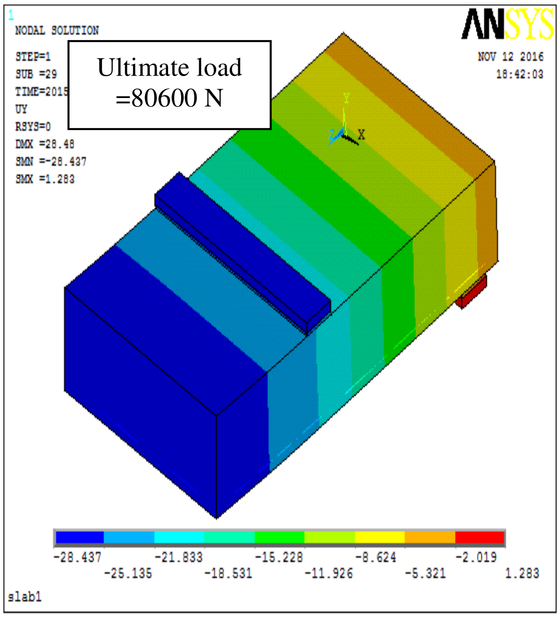

Figure-7. Deflection contours in y-direction of tested slab (1) at ultimate load.

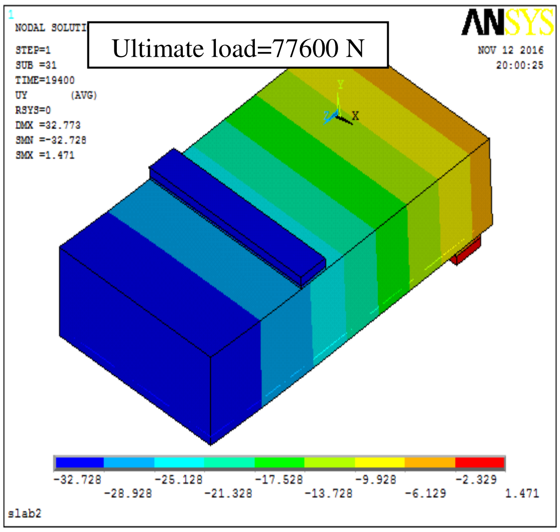

Figure-8. Deflection contours in y-direction of tested slab (2) at ultimate load.

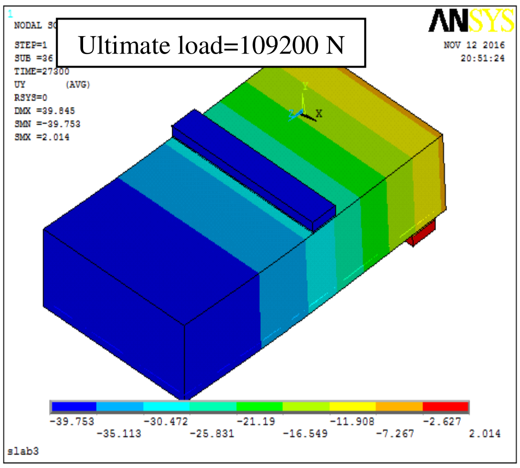

Figure-9. Deflection contours in y-direction of tested slab (3) at ultimate load.

 ISSN 1819-6608
ARPN Journal of Engineering and Applied Sciences

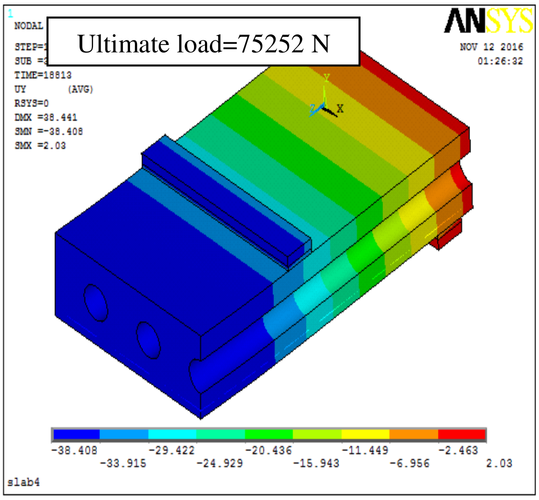

Figure-10. Deflection contours in y-direction of tested slab (4) at ultimate load.

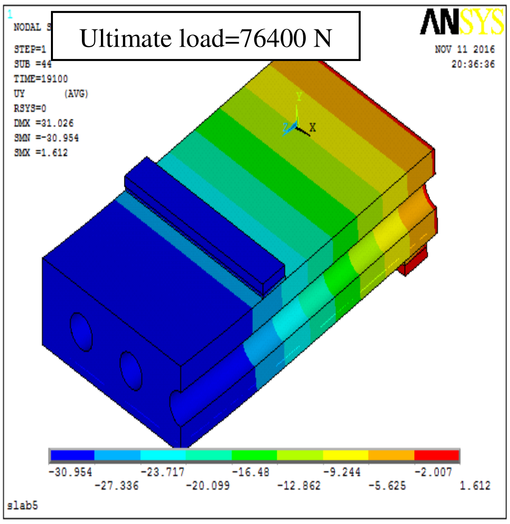

Figure-11. Deflection contours in y-direction of tested slab (5) at ultimate load.

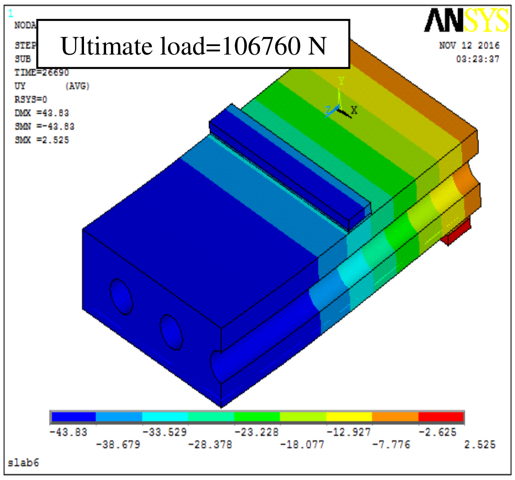

Figure-12. Deflection contours in y-direction of tested slab (6) at ultimate load.

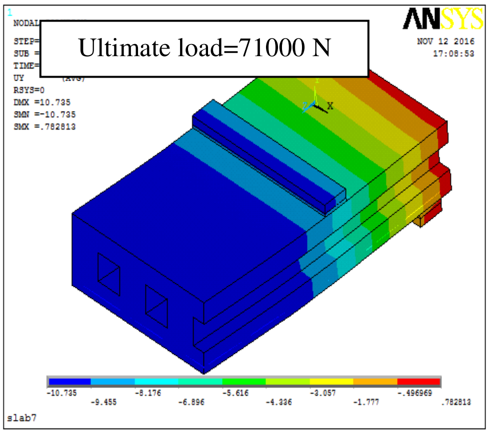

Figure-13. Deflection contours in y-direction of tested slab (7) at ultimate load.

The loads versus deflection plots obtained from numerical and experimental study are presented in Figures (14) to (20). The load-deflection curves of slabs show good correspond with the experimental test result. Results of comparison between experimental work and numerical analysis are in the range (3.05-10.5%) in ultimate load and (0.21-13.08) % in ultimate deflection value [12].

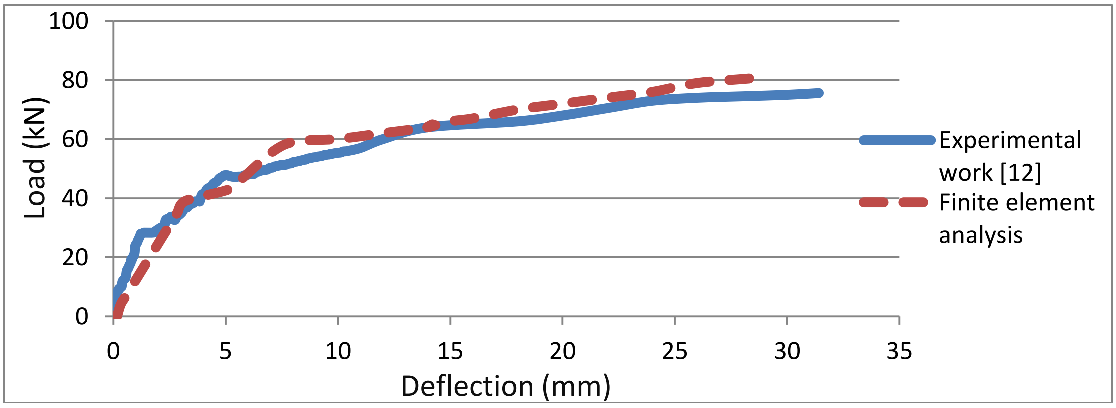

Figure-14. Experimental and finite element load - deflection curves for slab (1).

VOL. 12, NO. 6, MARCH 2017 ISSN 1819-6608
ARPN Journal of Engineering and Applied Sciences

www.arpnjournals.com

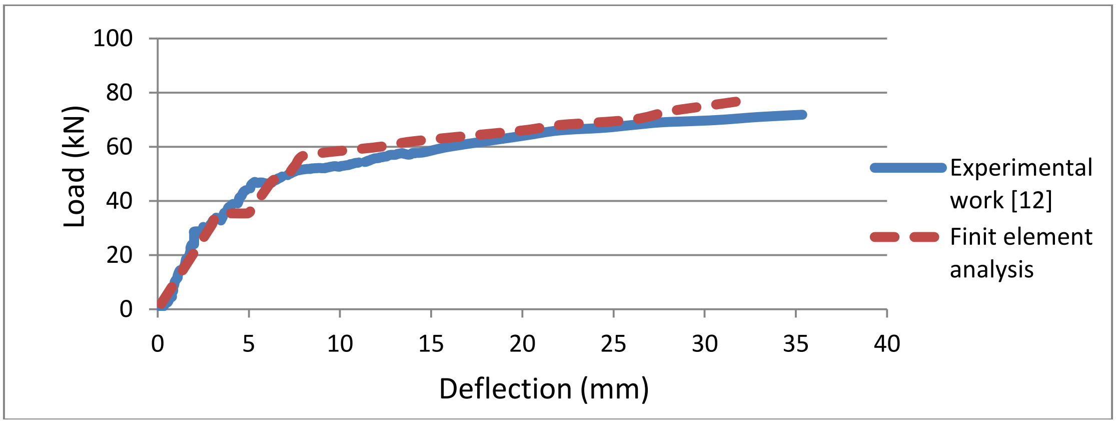

Figure-15. Experimental and finite element load - deflection curves for slab (2).

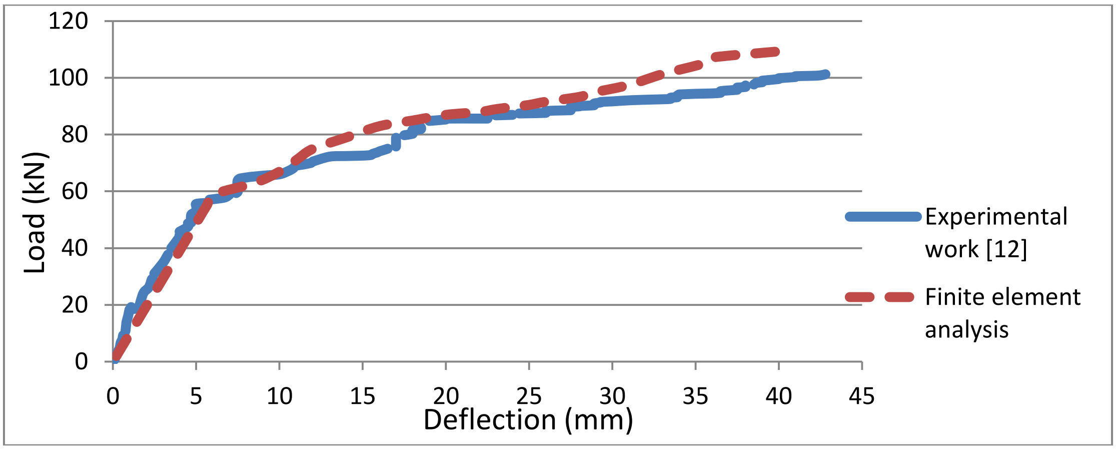

Figure-16. Experimental and finite element load - deflection curves for slab (3).

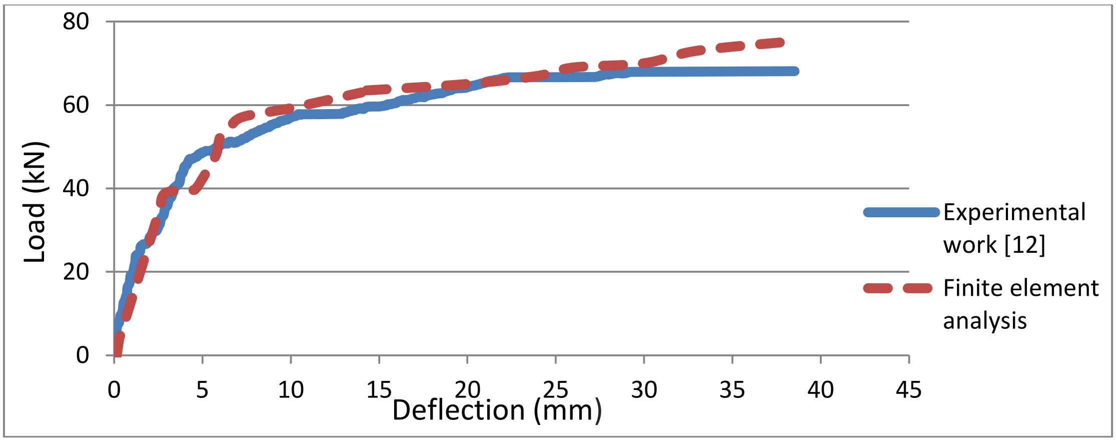

Figure-17. Experimental and finite element load - deflection curves for slab (4).

VOL. 12, NO. 6, MARCH 2017 ISSN 1819-6608
ARPN Journal of Engineering and Applied Sciences

www.arpnjournals.com

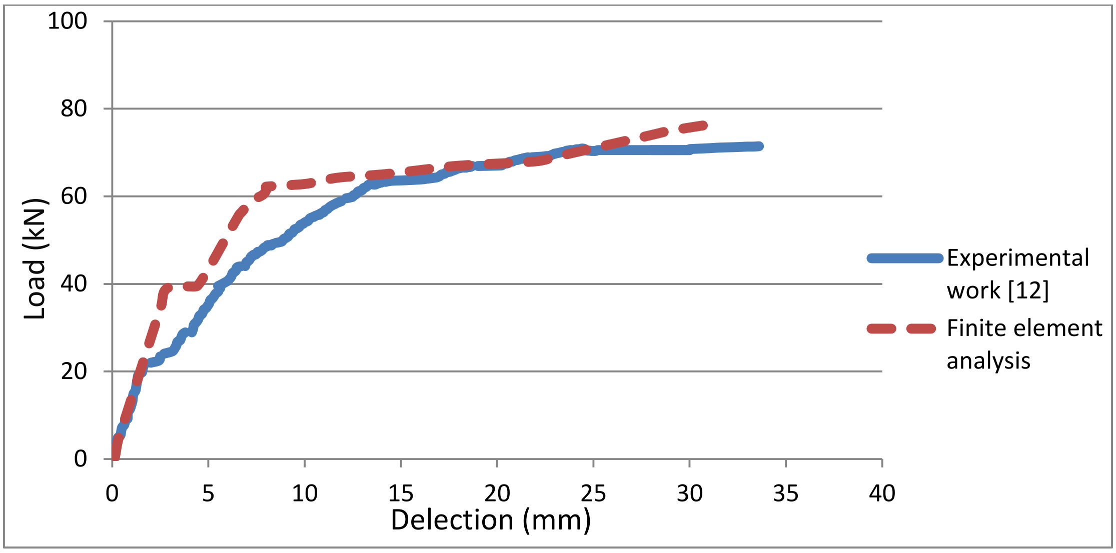

Figure-18. Experimental and finite element load - deflection curves for slab (5).

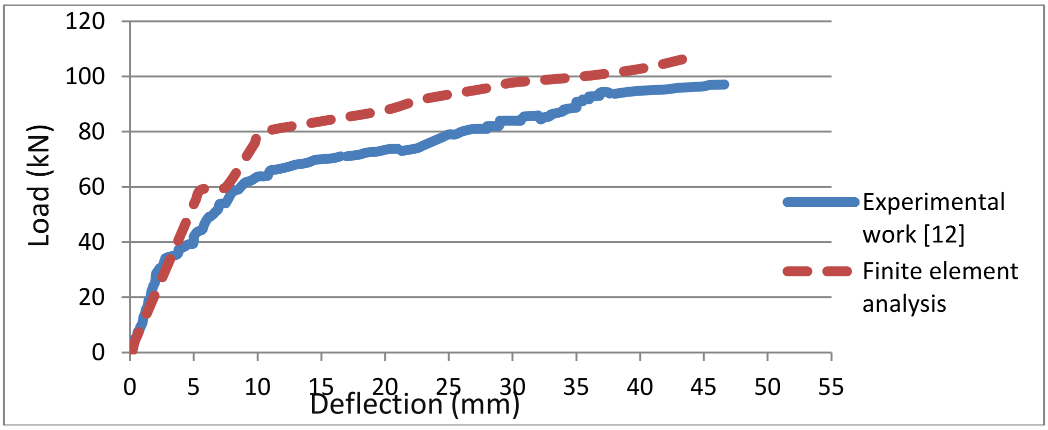

Figure-19. Experimental and finite element load - deflection curves for slab (6).

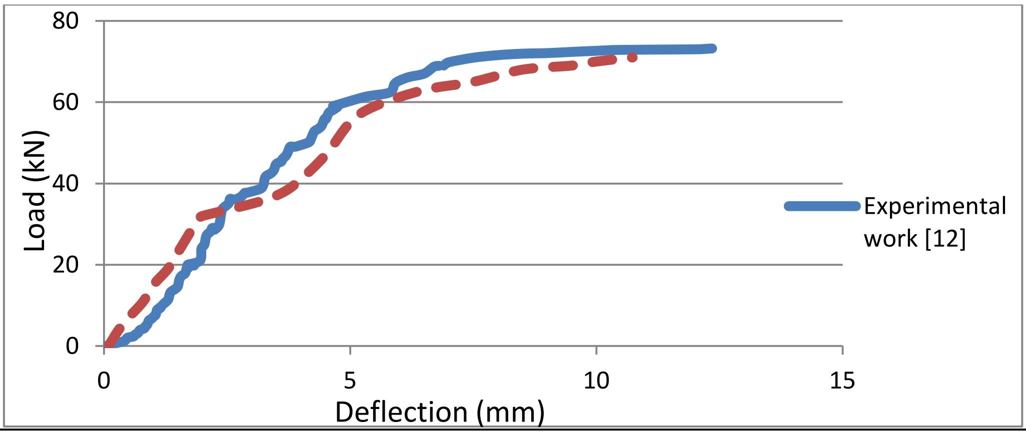

Figure-20. Experimental and finite element load - deflection curves for slab (7).

Stresses in reinforcing steel

3 The variation of normal stresses in steel reinforcement is shown in figures (21) to (23). All figures show that the steel reinforcement reached the yield stress near the mid span.

ISSN 1819-6608
ARPN Journal of Engineering and Applied Sciences

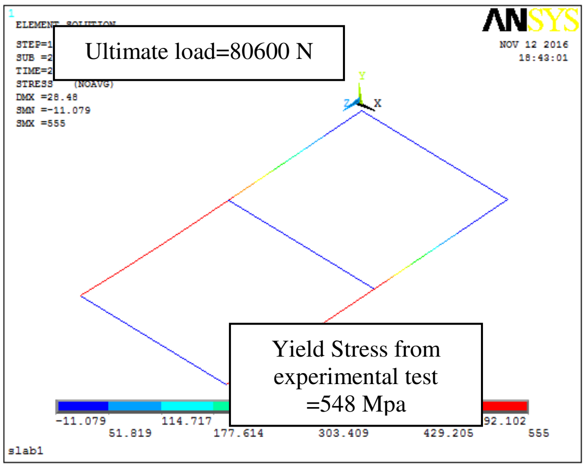

Figure-21. Stresses in longitudinal steel of slab (1).

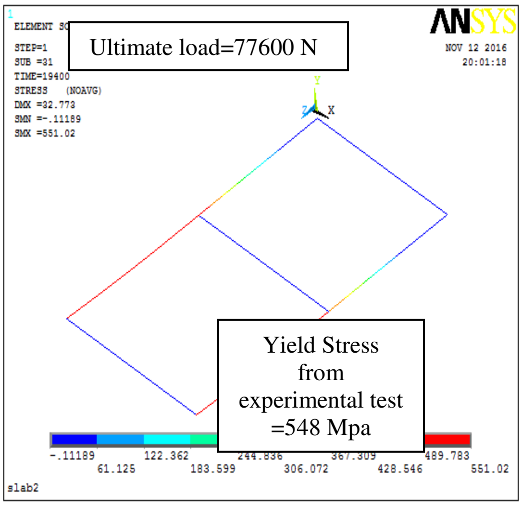

Figure-22. Stresses in longitudinal steel of slab (2).

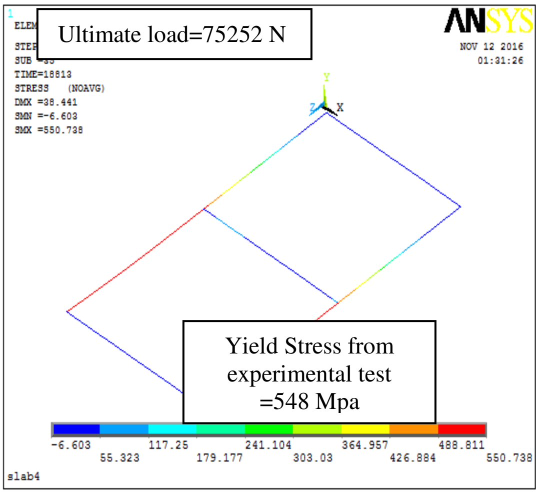

Figure-23. Stresses in longitudinal steel of slab (4).

Cracking patterns

The location of cracks and crushed points in the solid and hollow core slabs are shown in figures (24) to (28) ANSYS explain the cracks signs as shown in Table-8:

Table-8. Cracks signs of cracking patterns for specimens.

	First crack
	Second crack
	Third crack
	Represents the flexural crack
	Represents the diagonal tension crack
	Sign represents two cracks (the first crack is diagonal tension crack and the second crack with a green circle outline is compressive crack)
	Sign represents three cracks (the first and second cracks are diagonal tension cracks and the third crack with a blue circle outline is compressive crack).

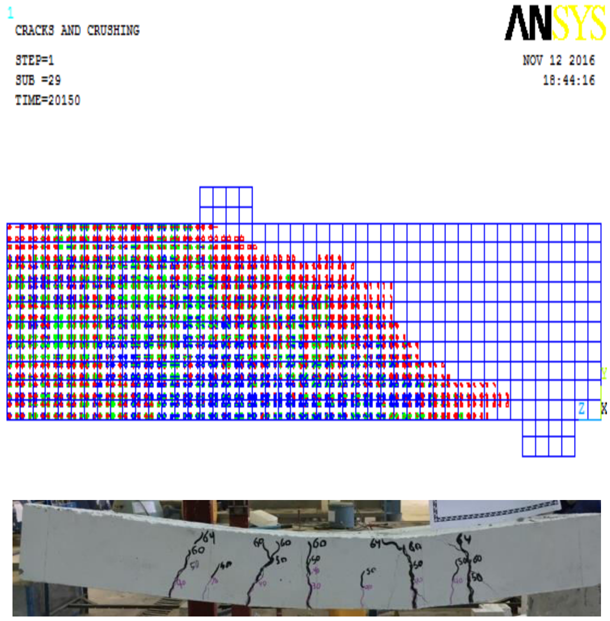

Figure-24. Crack pattern at failure for slab (1).

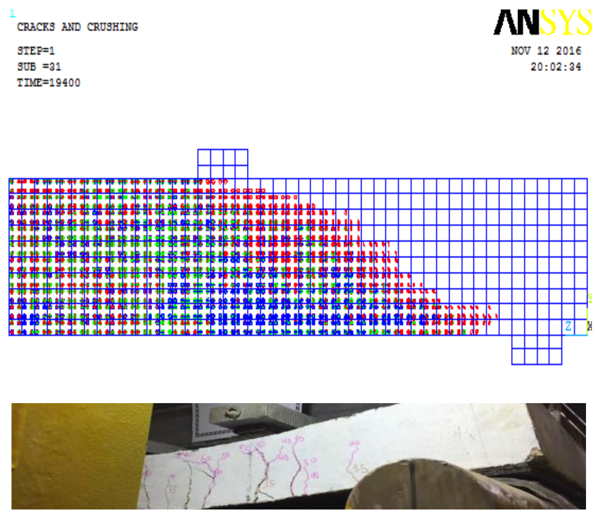

Figure-25. Crack pattern at failure for slab (2).

VOL. 12, NO. 6, MARCH 2017 ISSN 1819-6608
ARPN Journal of Engineering and Applied Sciences

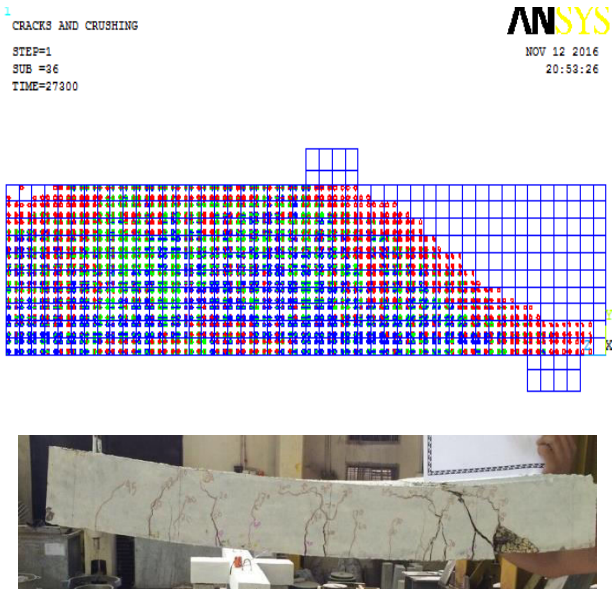

Figure-26. Crack pattern at failure for slab (3).

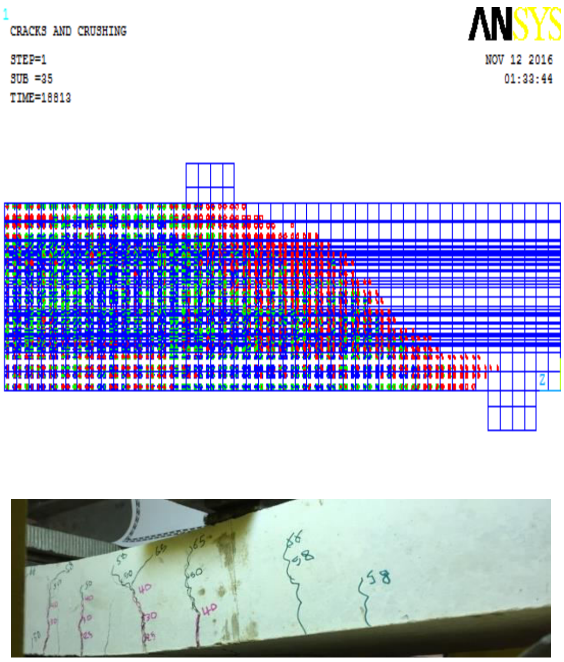

Figure-27. Crack pattern at failure for slab (4).

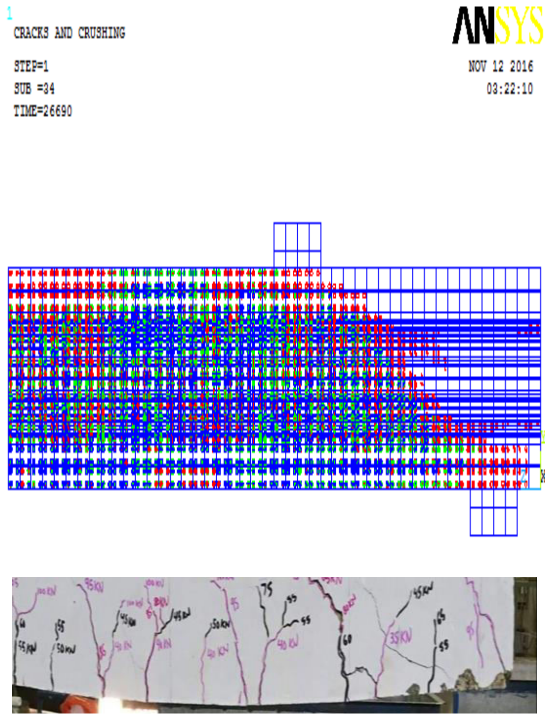

Figure-28. Crack pattern at failure for slab (6).

Parametric study

a) Effect of top layer of reinforcement

Figure-29 shows the effect of using top and bottom steel reinforcement. Slab4 is hollow circular core slab made with lightweight aggregate and core diameter (50mm) under two line loads with a/d equal (2.9) was analyzed first with only bottom reinforcement and then analyzed with top and bottom reinforcement with the same characteristic (bars diameter=8mm and yield stress=548). It was noted that the ultimate load and deflection values of the slab is increased by about 29.37% and 16.15% respectively for slab with top reinforcement (also it has flexural failure mode). This is may be due to the existence of top reinforcement will distribute the stresses around the core and prevent crushing of the concrete over the cores due to the increase in stresses.

VOL. 12, NO. 6, MARCH 2017 ISSN 1819-6608
ARPN Journal of Engineering and Applied Sciences

www.arpnjournals.com

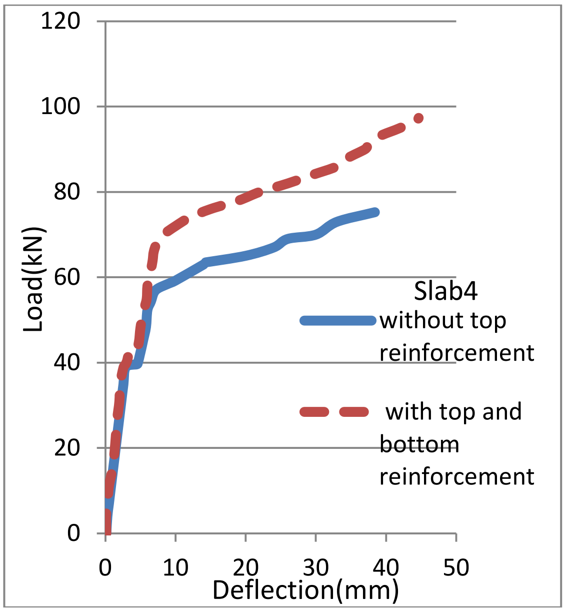

Figure-29. Effect of top layer of steel reinforcement on lightweight aggregate hollow circular core slab.

b) Effect of cores number

Slab4 (HCCS with LWA, a/d=2.9 and reduction in weight about 32.92%) is utilized to study the effect number of core on the load-deflection response. Slab4 was analyzed first with five cores and then the same slab is analyzed with only three cores. The load deflection curves for this slab are shown in Figure-30. It is found that the load-deflection behavior of slab with three cores is stiffer than those with five cores. The ultimate capacity was found to be greater for slabs with three cores than those with five cores by about 8.97% and also the deflection value is decreased when using three cores by about 10.77% but the reduction in weight decreased to become about 27.46% and it has flexural mode of failure.

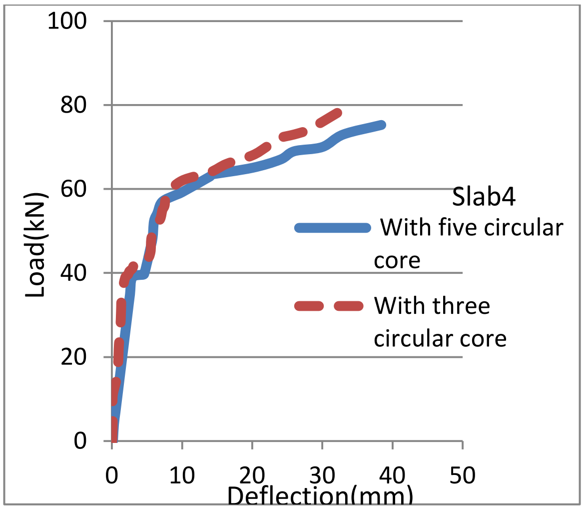

Figure-30. Effect number of cores on the behavior of lightweight aggregate hollow circular core slab (slab4).

c) Effect of core diameter

Slab4 (HCCS with LWA, a/d=2.9 and reduction in weight about 32.92%) is used to study the effect of changing the diameter of the core. Slab4 was analyzed first with cores diameter equal (50mm) and then the same slab is analyzed with cores diameter equal (70mm) (keeping number of cores constant). The load deflection curves for this slab are shown in Figure-31. It is found that the load-deflection behavior of slab with cores diameter equal (50mm) is stiffer than those with cores diameter equal (70mm). The ultimate capacity was found to be decreased for slabs with cores diameter equal (70mm) than those with cores diameter equal (50mm) by about 16.28% and also the deflection value is increased for cores diameter equal (70mm) by about 9.76% but the reduction in weight increased to become about 46% and mode of failure remains flexure.

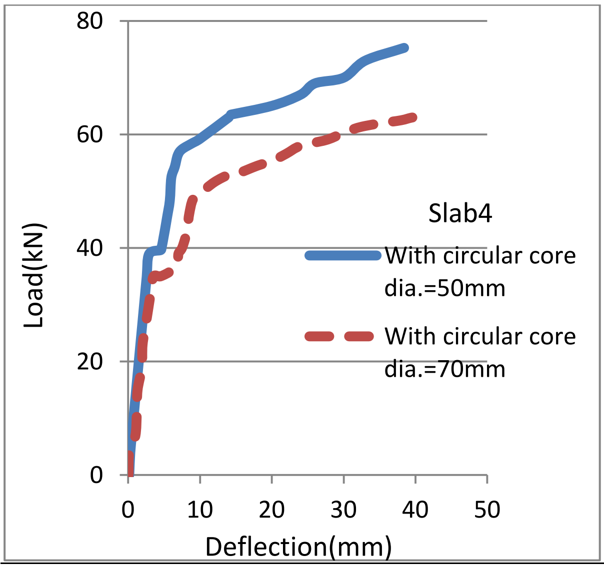

Figure-31. Effect of cores diameter in lightweight aggregate hollow circular core slab (slab4).

d) Effect of load location on the behavior of slab

Slab4 (HCCS with LWA and a/d=2.9) is used to study the impact of number of line load on the behavior of slabs. Slab4 was analyzed first using two lines loads and then the same slab is analyzed under one line load at the mid span slab. The load deflection curves for this slab are shown in Figure-32. Notice that when one line load at the mid span of slab is applied the ultimate load is close to ultimate load when two line loads are applied but the deflection value increased about10.82% and it has similar mode of failure.

ARPN Journal of Engineering and Applied Sciences

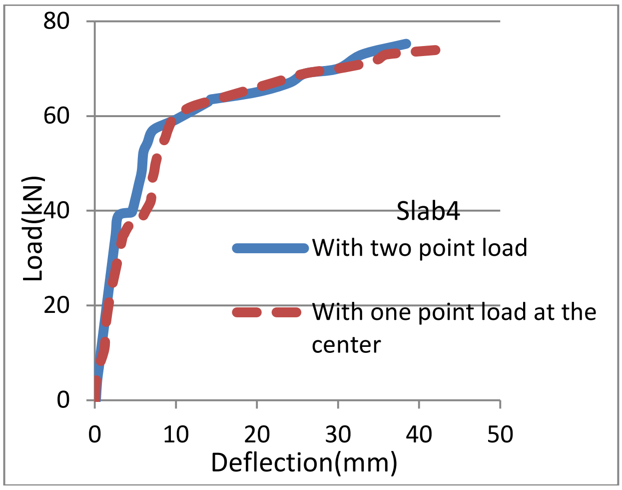

Figure-32. Effect of load location in lightweight aggregate hollow circular core slab (slab4).

e) Effect the distance between applied load location and supports

Slab4 (HCCS with LWA and a/d=2.9) and slab6 (HCCS with LWA and a/d=1.9) are used to study the effect of the distance between applied load location and supports on the behavior of slabs. Slab4 was analyzed under two line loads with a/d ratio equal (2.9) and slab6 was analyzed under two point loads with a/d ratio equal (1.9) but when analysis slab only quarter of model was used. The load deflection curves for this slab are shown in Figure-33. Notice that when a/d ratio increased from (1.9) to (2.9), the ultimate load decreased by 29.51% and also the deflection value is decreased by 12.3%.

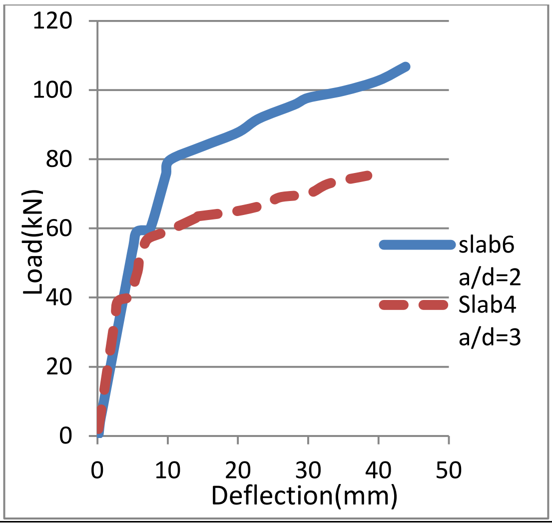

Figure-33. Effect of the distance between loads location and supports.

f) Effect of top reinforcement on shear behavior

Slab7 (HSCS with LWA and a/d=1.9) is used to study the effect of top reinforcement on shear behavior. Slab7 was failed due to shear in experimental work when tested with only bottom reinforcement. The slab with additional top reinforcement is used and analyzed using ANSYS program. The mode of failure was changed to flexural failure with smaller shear cracks. The load deflection curves for this slab are shown in Figure-34. When top reinforcement is used the ultimate load increased by about 24.87% and the deflection value at failure increased from 12.35mm to 35.12mm.

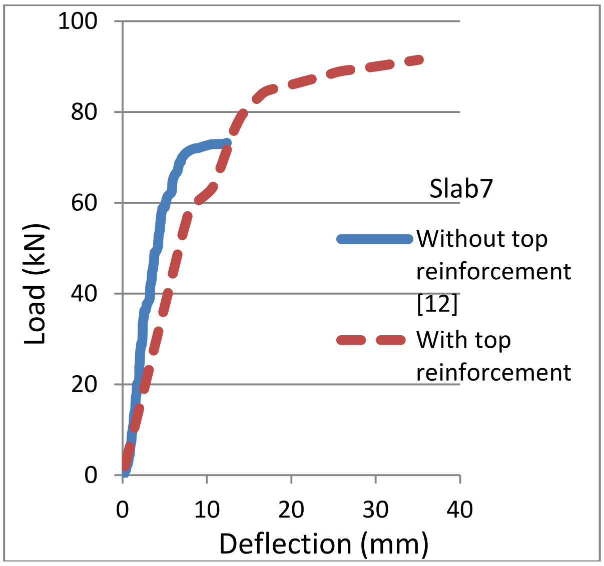

Figure-34. Effect of top reinforcement on shear behaviour.

CONCLUSIONS

The following main conclusions can be drawn:

a) The ultimate loads obtained from finite elements are in good agreement with experimental results with (7.56%) difference. The difference in ultimate deflection was (7.26%).

b) The crack patterns obtained from finite elements are in good agreement with experimental ones.

c) The effect of using top reinforcement for hollow circular core slab (a/d=2.9) is found to be significant. It was noted that the ultimate load and deflection increased by (29.37%) and (16.15%) respectively.

d) The effect of number of cores is found to be significant for hollow circular core slab (a/d=2.9). If the number of cores increased from 3 to 5 the ultimate load decreased by (8.97%) and the deflection is increased by (10.77%). The reduction in weight increased from (27.46%) to (32.92%).

e) The effect of core diameter is found to be significant for hollow circular core slab (a/d=2.9). If the core diameter increased from (50mm) to (70mm), the ultimate load is decreased by (16.28%) and the deflection is increased by (9.76%).

f) When applied one line load at the mid span of lightweight aggregate hollow circular core slab the ultimate load is close to ultimate load when two line loads are applied but the deflection value increased about10.82% and it has similar mode of failure.

g) Increasing the (a/d) ratio from 1.9 to 2.9 causes to reduce the strength capacity about (29.51%) in

ARPN Journal of Engineering and Applied Sciences

lightweight aggregate hollow circular core slab with decreasing in deflection value about (12.3%).

h) The effect of top reinforcement is found to be significant on ultimate loads and deflection by (24.87%) and (35.12%) respectively for hollow square core slab. The mode of failure change from shear to flexure.

REFFRENCES

[1] Holm Thomas A. 1995. Lightweight Concrete and Aggregate. Standard Technical Publication STP 169c. pp. 522-532.

[2] Fadia S. Kallak. 2009. Use of Crushed Bricks as Coarse Aggregate in Concrete. M.Sc. Thesis, Civil Eng. Dept, University of Tikrit.

[3] Osama M. Ghazi. 2011. Properties of Hardened Concrete Using Crushed Clay Brick as Aggregate. Assis.lec. AI-Mustansireah University, College of Engineering - Civil Department. Vol. 17.

[4] Yousif K. Yousif. 2016. Behavior of Structural Lightweight Self Compacted Reinforced Concrete Thick Slabs under Static Loading. D.Sc. Thesis, Civil Eng. Dept, University of Al-Nahrain.

[5] Al-Maleki M. M. 2006. Analysis oh Hollow Core Reinforce Concrete Slabs Subject to Applied Loads. M.Sc. Thesis, Civil Eng. Dep., Nahrain University.

[6] Donald R. Buettner and Roger J. Becker Computerized Structural Design, S.C.PCI. 1998. Manual for the Design of Hollow Core Slabs. 175 West Jackson Boulevard Chicago, Illinois 60604 312 786-0300.

[7] Qaqish M., Akawwi E. and Fadda E. 2009. Comparison Between Computed Shearing Forces by AASHTO Specifications and Finite Element Method of Two Continuous Spans of Voided Slab Bridge‖, WSEAS Transactions on Information Science and Applications. 6(4).

[8] Mahdi A. S. 2011. Nonlinear Finite Element Analysis of Reinforced Concrete Hollow Core Slabs. MSc. Thesis, Al-Nahrain University /Civil Engineering Department.

[9] Adel A. Al-Azzawi and Sadeq A. Abed. 2016. Numerical Analysis of Reinforced Concrete Hollow-Core Slabs. ARPN Journal of Engineering and Applied Science. 11(15).

[10] ANSYS. 2011. ANSYS Manual. V. 11.0 Releases.

[11] Willam K.J. and Warnke E.P. 1974. Constitutive Model for Triaxial Behavior of Concrete. Seminar on Concrete Structures Subjected to Triaxial Stressed, International Association of Bridge and Structural Engineering Conference, Bergamo, Italy. p. 174.

[12] Basma M. Abdul Al-Aziz. 2017. Analysis of Reinforced Lightweight Aggregate Concrete Hollow Core Slabs. M.Sc. Thesis, Civil Eng. Dept, University of Al-Nahrain.